

Automated Mapping of Surface Water Temperature in the Great Lakes*

David J. Schwab**, George A. Leshkevich, and Glenn C. Muhr

NOAA Great Lakes Environmental Research Laboratory
2205 Commonwealth Blvd.
Ann Arbor, Michigan 48105

ABSTRACT. A procedure for producing daily cloud-free maps of surface water temperature in the Great Lakes has been developed. It is based on satellite-derived AVHRR (Advanced Very High Resolution Radiometer) imagery from NOAA's CoastWatch program. The maps have a nominal resolution of 2.6 km and provide as complete as possible coverage of the Great Lakes on a daily basis by using previous imagery to estimate temperatures in cloud covered areas. Surface water temperature estimates derived from this procedure compare well with water temperatures measured at the eight NOAA weather buoys in the lakes. The mean difference between the buoy temperature and the satellite-derived temperature estimates is less than 0.5°C for all buoys. The root mean square differences range from 1.10 to 1.76°C.

As one example of the possible applications of this product, the daily surface water temperature maps for 1992 to 1997 were analyzed to produce daily estimates of average surface water temperature for each lake. Results are compared to the long-term (28 year) mean annual cycle of average surface water temperatures. The average surface water temperatures vary from as much as 4°C below climatology in 1993 to 2 to 3°C above climatology in 1995. The new analysis procedure also provides a more realistic depiction of the spatial distribution of temperature in the springtime than the climatological maps.

INDEX WORDS: Water temperature, satellite, AVHRR, climatology, seasonal variation, Great Lakes.

INTRODUCTION

Water temperature has a profound influence on the entire aquatic ecosystem as well as on the wide variety of human activities in the Great Lakes. In addition, because the Great Lakes contain a sufficiently large volume of water with sufficiently large areal extent, the surface water temperatures can exert a significant influence on regional weather patterns (Petterson and Calabrese 1959, Lyons 1971). For these reasons, as well as for monitoring climatological temperature conditions in the lakes, knowledge of the spatial and temporal distribution of lake surface water temperature can be extremely valuable.

Historically, routine water temperature measurements have been obtained at locations of opportunity such as municipal water intakes (McCormick and Fahnenstiel 1998) and water level gauging sta-

tions (Grumblatt 1976). Unfortunately, because of the high variability of water temperature in nearshore zones and their limited spatial coverage, they are not adequate for resolving the spatial distribution of temperature in the lake. Since 1979, the NOAA National Data Buoy Center (NDBC) has operated a series of satellite-reporting weather buoys in the Great Lakes during the ice-free season, generally from April to December (Hamilton 1986). Lesht and Brandner (1992) used water temperature measurements from the NDBC buoys to derive climatological curves for the annual cycle of water temperature variation at the buoy locations. The offshore location of the buoys provides water temperatures which are more representative of lakewide averages, but still not sufficient for describing spatial variability.

In order to obtain information about lakewide temperature distribution patterns, several early investigators mounted ship-based synoptic surveys of the lakes (Church 1945, Ayers 1965, Anderson and

*GLERL Contribution Number 1118

**Corresponding author E-mail: schwab@glerl.noaa.gov

Rodgers 1963). Later, aircraft-mounted radiation thermometers were used to map surface temperature distribution in several of the lakes (McFadden and Ragotzkie 1963, Webb 1974, Weiss 1970, Irbe 1992). Neither ship nor aircraft-based surveys are practical for routine (daily) mapping of lake surface water temperature, mainly because of the large size of the lakes and the resources involved.

More recently, infrared imaging sensors on weather satellites were found to be an excellent tool for obtaining both spatial and temporal distribution of surface water temperature (Strong 1974, Irbe *et al.* 1979, Bolgrien and Brooks 1992, Schwab *et al.* 1992). Schneider *et al.* (1993) combined a large number of water temperature maps derived from air-borne and satellite-borne radiometers with the ice cover climatology developed by Assel *et al.* (1983) to produce a combined water temperature and ice climatology for the Great Lakes. Computerized maps of "normal" water temperature and ice cover were generated for each day of the year. They also used a numerical model to estimate representative vertical temperature profiles for each lake. However, the methodology used to create the climatological water temperature and ice distributions was not amenable to routine automated operation.

The purpose of this paper is to describe a routine automated technique for using satellite imagery to derive a complete map of Great Lakes surface water temperature based on satellite imagery on a daily basis. The technique uses near real-time SST (sea surface temperature) imagery and cloud mask maps for the Great Lakes from the NOAA CoastWatch program (Schwab *et al.* 1992, Leshkevich *et al.* 1997), so that the automated maps can be produced in near real-time. Temporal and spatial interpolation are employed to fill in gaps caused by cloud cover or other problems.

As one example of the potential applications for this product, a summary of the daily GLSEA (Great Lakes Surface Environmental Analysis) temperature maps from 1992 to 1997 is presented in the form of lakewide average surface water temperature time series for each lake. Lakewide average temperatures have commonly been used in bulk hydrological and ecological models, but aside from hydrodynamic modeling results and single point measurements from weather buoys, no information on lake average surface water temperature has been routinely available. Water temperatures from the GLSEA images are also compared to single point time series from the NOAA weather buoys as well as to lake average climatological values.

METHODS

Satellite Imagery

The NOAA CoastWatch program was developed in 1990 to provide access to NOAA satellite imagery in support of coastal management and research activities (Pyke 1989, Schwab *et al.* 1992). Most of the products available through this program are based on imagery from the AVHRR (Advanced Very High Resolution Radiometer) instrument aboard NOAA's polar orbiting weather satellites. The polar orbiting satellites are in a sun-synchronous orbit at an altitude of approximately 833 km which allows them to pass over a given area of the earth twice a day. There are generally two polar orbiting satellites in operation, resulting in four possible images per day for a given area. The AVHRR scans a swath of approximately 2,700 km width on the earth's surface beneath the satellite using five radiometric bands (0.58–0.68 μ , 0.725–1.0 μ , 3.55–3.93 μ , 10.3–11.3 μ , 11.5–12.5 μ) (Kidwell 1995). The AVHRR data are processed at NESDIS (National Environmental Satellite and Data Information Service) for the CoastWatch program to generate a 512 \times 512 pixel image of the entire Great Lakes region on a Mercator geographic projection at approximately 2.6 km resolution and three 512 \times 512 pixel subscenes of the northern, western, and eastern parts of the Great Lakes region at 1.3 km resolution. There are separate files for data from each radiometric band, as well as satellite and solar zenith angle, cloud mask, and an estimate of sea surface temperature derived from the radiometric data (Leshkevich *et al.* 1993).

Geographic Registration

The 512 \times 512 images in the Great Lakes region are based on a Mercator projection with fixed corner points. Because of satellite navigation and timing errors, an individual satellite image is usually not exactly registered with fixed landmarks in the Mercator window. Bordes *et al.* (1992) discuss the sources of navigation errors and describe a procedure they developed for automatic adjustment of AVHRR imagery over Europe. Here it was found that, for the Great Lakes image, errors can be as large as 10 km. Therefore, an automated procedure for georeferencing each full regional Great Lakes scene was developed. In order for the procedure to be completely automatic, three assumptions were made: 1) It was assumed that the navigation errors in the 512 \times 512 CoastWatch image can be cor-

rected by a linear translation of the image by an integral number of pixels in the north-south and east-west directions. Although this is not always true, errors remaining in the linearly transposed image rarely exceed 2.6 km (one pixel); 2) It was assumed that there is sufficient cloud-free area in the image so that a significant section of the shoreline can be distinguished. If this is not the case, the image cannot be georeferenced; 3) It was assumed the linear correction will not exceed five pixels in either direction from a starting point based on the average translation of images from this satellite over the previous few weeks. If the linear correction is more than five pixels, the image cannot be georeferenced. This assumption can potentially be relaxed by increasing the range of the linear correction, but only at the expense of increased computer processing time.

In order to implement this algorithm for both daytime and nighttime imagery, the 5-lake SST image was used, which is available for all satellite passes. The CoastWatch SST file for this image is uncompressed and decoded and the temperature in the image is scaled to an eight bit pixel value ranging from 0 to 255. To maximize the contrast in the image, the scaled temperature range varies throughout the year. For days of the year 1 to 99 and 320 to 365, the range is -10°C to 20°C . For days 100 to 137 and 283 to 319, the range is -5°C to 25°C . For days 138 to 282, the range is 0 to 30°C . The digital image is then processed with a Roberts edge detection filter:

$$g_{i,j} = |f_{i,j} - f_{i+1,j+1}| + |f_{i,j+1} - f_{i+1,j}| \quad (1)$$

where $g_{i,j}$ is a pixel in the enhanced image and $f_{i,j}$ is a pixel in the original image. This process generates large values in regions where the image intensity (temperature) changes abruptly. It was found that it works very well for detecting the lake shorelines. After the edge detection filter has been applied to the image, a threshold value is calculated for the histogram of the enhanced image such that one third of the pixels in the image have values less than the threshold and two thirds have greater values. Pixels with values less than the threshold are set to zero and pixels with values greater than the threshold are set to one. This procedure tends to enhance the strong gradients near the shorelines and to eliminate the smaller gradients over land or water. Since navigation errors in satellite positioning tend to be persistent with time, the enhanced image is first shifted by the number of east-west

and north-south pixels corresponding to the average geocorrection for this satellite over the past few weeks. This provides an initial guess for the linear geocorrection. Then a correlation is calculated between an image of known shoreline locations (shoreline pixels = 1, land and water = 0) and the pixels in the enhanced image with values greater than the threshold. The correlation is also calculated for all linear displacements of the enhanced image of up to ± 5 pixels in either direction. The optimum linear displacements for this image are those for which the correlation with the known shoreline image is a maximum. This correction is applied to the original temperature image, and the east-west and north-south displacements for the image are recorded for future reference. The georeferencing procedure does not currently include provisions for detecting nearshore ice, but this could possibly be included in the future.

Cloud Masking

In 1994, a cloud mask for CoastWatch AVHRR imagery based algorithms developed by Stowe *et al.* (1991) and adapted for use in the CoastWatch program by Maturi and Pichel (1993) was included as part of the CoastWatch product suite. The algorithms consist of seven different tests for daytime images and five tests for nighttime images as shown in Table 1. If a pixel fails any of these tests except the Thermal Uniformity Test, it is discarded from further processing. The Thermal Uniformity Test was not used as it was found to be overly restrictive for use in the Great Lakes. An example of the results of the six cloud mask tests used for the daytime NOAA 14 AVHRR image on JD 228, 1995 is shown in Figure 1. In this particular image, Reflective Gross Cloud Test (Test 1) and the Reflective Uniformity Test (Test 2) are the most restrictive.

In 1992–93, before the CoastWatch cloud mask files were available, the following procedure based on AVHRR visible reflectance channels 1 and 2 was used to estimate which pixels are cloud-covered. If the channel 1 over-water reflectance was greater than 4% or the ratio of channel 2 to channel 1 reflectance was greater than 0.75, the pixel was considered cloud-covered. Next, if the SST was less than 0 for a pixel, it was masked. Since this procedure used reflectance channels 1 and 2, it was only applied to daytime images.

After cloud masking, all remaining pixels are used to compute an average and a standard deviation for the 3×3 pixel box around each pixel. If a

TABLE 1. Tests used in CoastWatch cloud mask product.

Bit	Cloud Mask Test	Channels Used	Threshold Value
Daytime Cloud Mask			
1	Reflective Gross Cloud Test	2	> 20%
2	Reflective Uniformity Test	2	> 0.3%
3	Reflectance Ratio Cloud Test	1, 2	$0.9 < R < 1.1$
4	Channel 3 Albedo Test	3, 4, 5	> 3%
5	Thermal Uniformity Test	4	> 0.5 degrees K
6	Four-minus-Five test	4, 5	> F(T4)
7	Thermal Gross Cloud Test	4	< 271 K
Nighttime Cloud Mask			
1	Thermal Gross Cloud Test	4	< 271 K
2	Thermal Uniformity Test	4	> 0.5 degrees K
3	Uniform Low Stratus Test	3, 5	< F(T4)
4	Four-minus-Five test	4, 5	> F(T4)
5	Cirrus Test	3, 5	< F(T4)

pixel has no cloud-free neighbors, it is masked. If the standard deviation of SST is greater than 3°C, the pixel is masked. Unmasked pixels are replaced by the 9 pixel average to smooth any high frequency noise in the image. The images are then land-masked so that only overwater pixels are considered.

Compositing

To form a composite temperature map, the pixels that pass the above screening tests are overlaid on the composite map from the previous day, but only if their total area within each lake is at least 5% of the surface area of the lake. If the number of valid pixels for a lake is greater than 20% of the lake area, then the average temperature for the valid area is computed both from the new pixels and from the composite from the previous day. All pixels for this lake in the composite from the previous day are adjusted by the difference between these average values. The new composite scene is smoothed with a 9 point average. Finally, the current daily composite scene is averaged with the composite scenes from the previous four days to create a 5-day composite. It was found that the 5-day average provided more realistic day-to-day temperature changes than the individual composite scenes, especially during transitions from cloudy to clear conditions. It was also found that during the winter and early spring season there are some areas where new temperature imagery may not be available for as long as 30 to 40 days because of cloud cover. During the summer, the longest an area usually goes without updating is

8 to 10 days. Water temperature from 0 to 30°C is scaled to digital pixel values 50 to 200. The pixel values are inserted into a background map and the resulting digital image is then made available as a Graphics Interchange Format (GIF) file. The daily automated processing for the GLSEA product is normally scheduled at 11:00 GMT (6:00 EST) on the day following the imagery acquisition in order to assure that all available imagery for that day has been processed by NESDIS and downloaded. The GLSEA product from the previous day is usually available by 6:30 EST. As noted above, the resolution of the water temperature data in the GLSEA product is 0.2°C (30 °C/150 counts), but in the GIF file, only 30 unique colors are assigned to the 150 count values in 1°C (5 count) increments. It is still possible to recover the 0.2°C resolution temperature values from the GIF file with any software which can access individual pixel values, i.e., water temperature (°C) = (pixel value – 50) / 5.

RESULTS

Comparison with NDBC Buoys

Since 1979, the NOAA National Data Buoy Center has operated a series of satellite-reporting weather buoys in the Great Lakes during the ice-free season, generally from April to December (Hamilton 1986). Data from eight buoys whose locations are shown in Figure 2 were available for each of the years 1992 to 97. The buoys carry a water temperature sensor on their hull approximately 1 m below the water surface. Although the

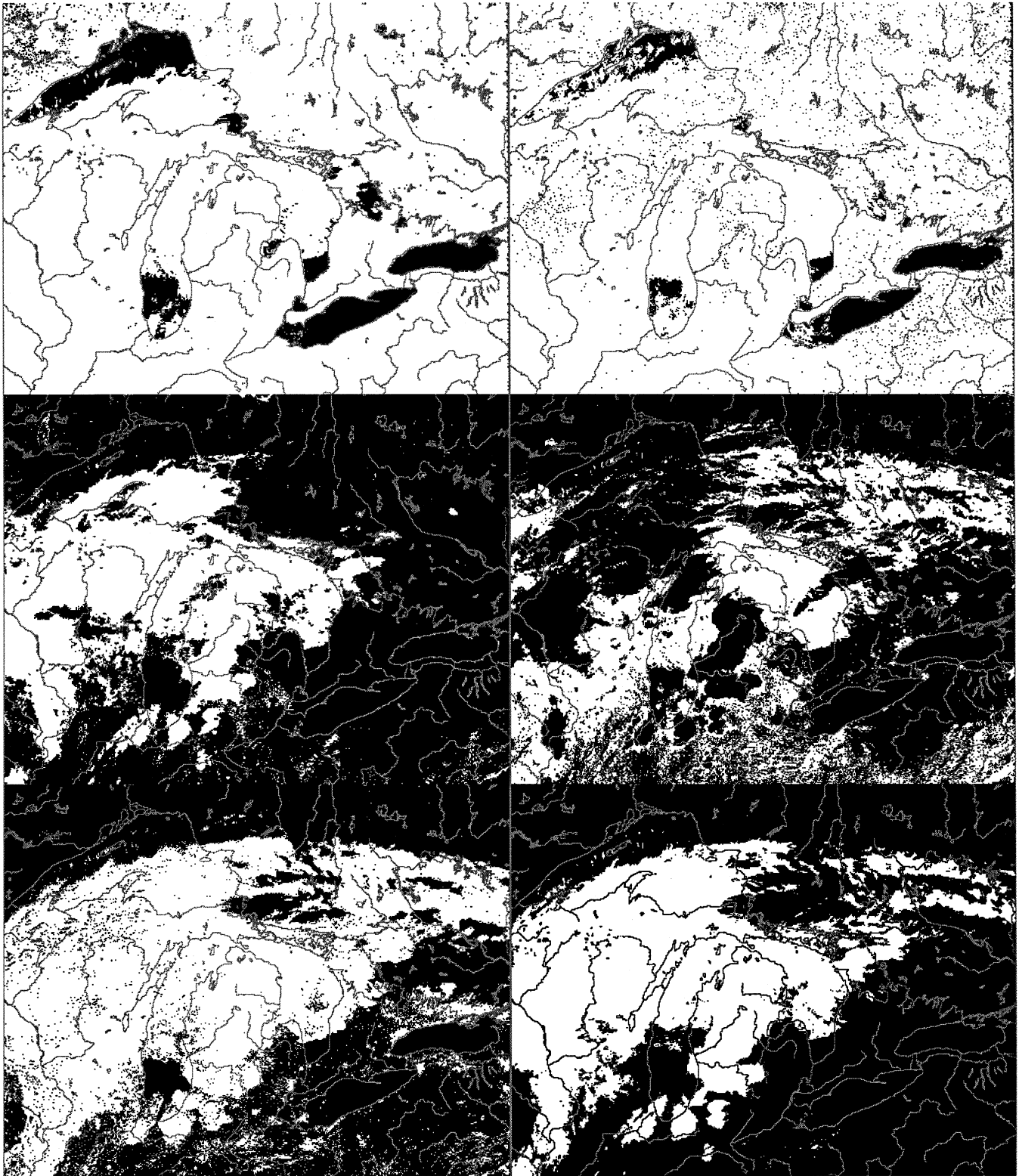


FIG. 1. Cloud mask examples. White areas indicate a positive result of the individual tests. The six panels (left to right, top to bottom) correspond to the daytime tests indicated in Table 1, excluding Test 5, the Thermal Uniformity Test. Upper left: Reflective Gross Cloud Test. Upper right: Reflective Uniformity Test. Center left: Reflectance Ratio Cloud Test. Center right: Channel 3 Albedo Test. Lower left: Four-minus-Five test. Lower right: Thermal Gross Cloud Test.

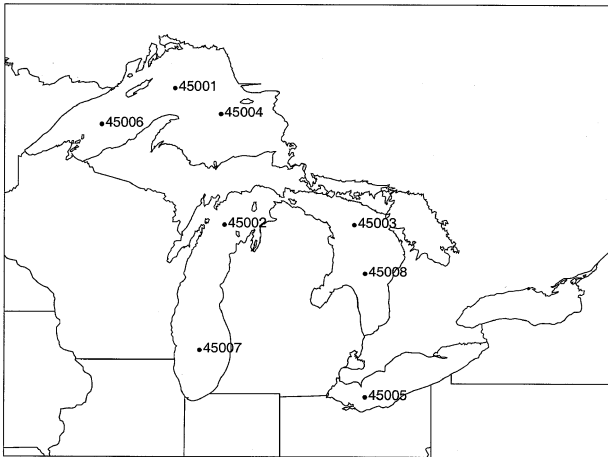


FIG. 2. Location of NOAA National Data Buoy Center (NDBC) weather buoys in the Great Lakes.

temperature measured by this sensor is not exactly comparable to the satellite-derived skin temperature, it should be very close (1°C or less) for typical conditions encountered in the lakes (Wesely 1979).

GLSEA water temperatures for the pixel nearest to each buoy were extracted from all the 5-day average daily composite maps produced from 1992 to 97. These data were then compared to daily average NDBC buoy temperature for all days when the buoy was operating. The results of the comparison are presented as scatter plots in Figure 3 and the statistical comparison is summarized in Table 2. The mean difference between the buoy temperature and the GLSEA temperature is less than 0.5°C for all buoys. The root mean square difference (RMSD) ranges from 1.10 to 1.76°C . Correlation coefficients (CC) are above 0.96 for all buoys.

GLSEA and Animations

Table 3 summarizes the history of GLSEA production. When the program was initiated in 1994, it was based only on NOAA 11 satellite imagery. The automated cloud mask product was not yet available, so only daytime imagery and a simple brightness thresholding procedure for cloud masking were used. In 1995, the automated cloud mask product allowed for inclusion of nighttime SST imagery into the algorithm. The NOAA 12 satellite was the only source of SST imagery from September, 1994 to March, 1995. NOAA 12 was not optimal for SST imagery because its orbit was

synchronized too close to the day-night terminator, which created problems with sun glint and made it difficult to develop consistent SST algorithms. Since April, 1995, NOAA 14 has been the primary source of SST and cloud mask imagery for the program.

Figure 4 shows an example of the GLSEA product for 29 May 1996. At this time, surface temperatures in Lake Erie and Saginaw Bay are already above 10°C in most areas, while the open parts of Lake Huron and the other lakes are still below 5°C . The thermal bar is developing in the southern part of Lakes Michigan and Huron. For comparison, Figure 5 shows the Daytime NOAA 14 AVHRR SST imagery on 29 May 1996 that was used in generating the GLSEA product. All of the main features in the SST image are reflected in the GLSEA map in Figure 4.

Figure 6 is another example of the GLSEA product from 16 August 1995 when water temperatures exceeded 25°C in all the lakes except Lake Superior. Even in Lake Superior, some areas had temperatures greater than 20°C . Figure 7 is the daytime NOAA 14 AVHRR SST image for 16 August 1995. This example shows how the GLSEA compositing process can provide useful maps of surface water temperature, even on cloudy days.

Figure 8 shows a third example of the GLSEA product for the same day as Figure 6, but for the previous year. Surface water temperatures in 1994 were 5 to 10°C cooler than in 1995.

At the end of each year, the daily GLSEA files are assembled into a computer animation for that year. The animation is useful for quickly examining the development of thermal structure for all five lakes.

Comparison with Climatology

As one example of the potential applications for the GLSEA product, the mean surface water temperature for each of the five Great Lakes was calculated for all the daily GLSEA maps from 1992 to 97. These values are plotted in Figure 9 and summarized as annual averages in Table 4. The daily climatological surface water temperature maps of Schneider *et al.* (1993) can also be used to calculate daily climatological average surface water temperatures. This annual climatological surface water temperature cycle is also plotted as a gray line in Figure 9. Figure 10 shows the departure of the daily GLSEA-derived temperature from the climatologi-

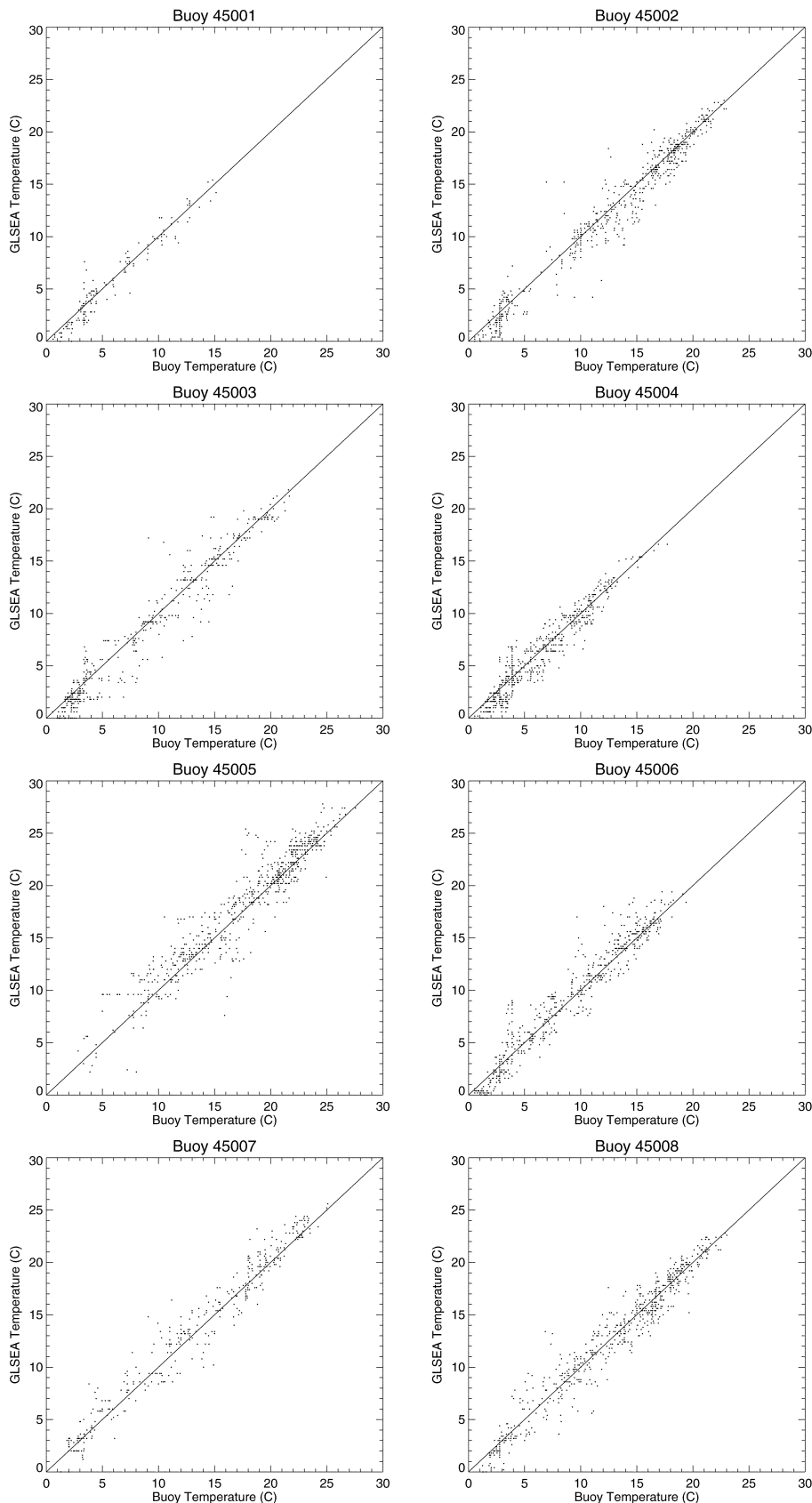


FIG. 3. Comparison of daily average water temperature at NDBC buoy locations in GLSEA maps to temperature measured by buoys.

FIGS. 4–8. (Facing page) **FIG. 4** (Upper left in color plate). GLSEA product for 29 May 1996.

FIG. 5 (Upper right in color plate). CoastWatch AVHRR SST image for 29 May 1996.

FIG. 6. (Middle left in color plate). GLSEA product for 16 August 1995.

FIG. 7 (Middle right in color plate). CoastWatch AVHRR SST image for 16 August 1995.

FIG. 8 (Lower left in color plate). GLSEA product for August 16, 1994.

FIG. 11 (Lower right in color plate). Climatological surface water temperature map from Schneider et al. (1993) for 29 May.

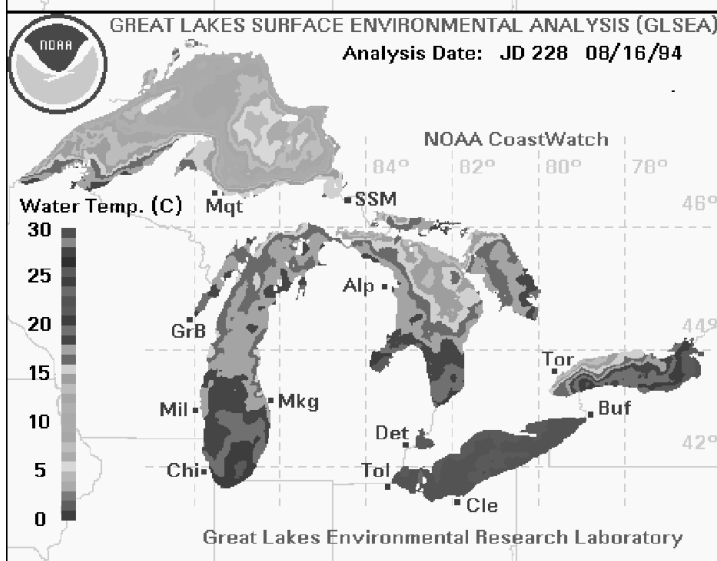
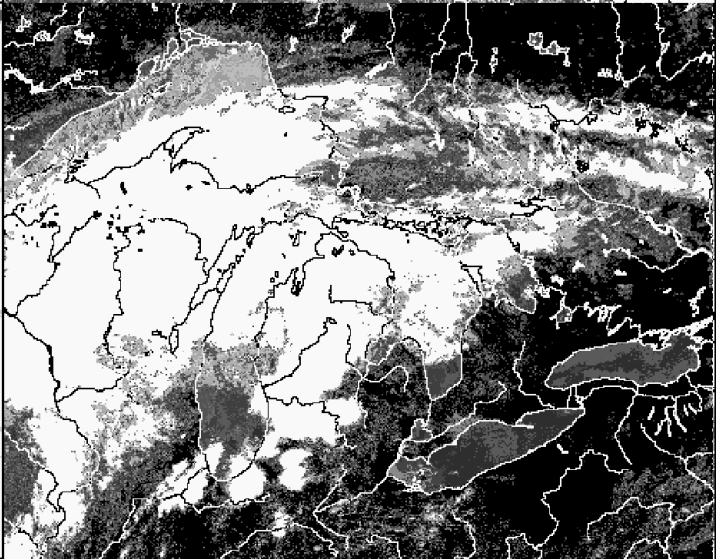
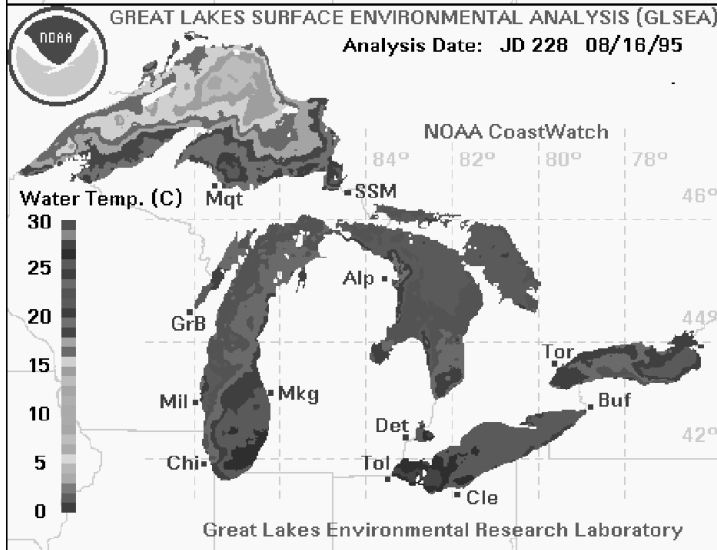
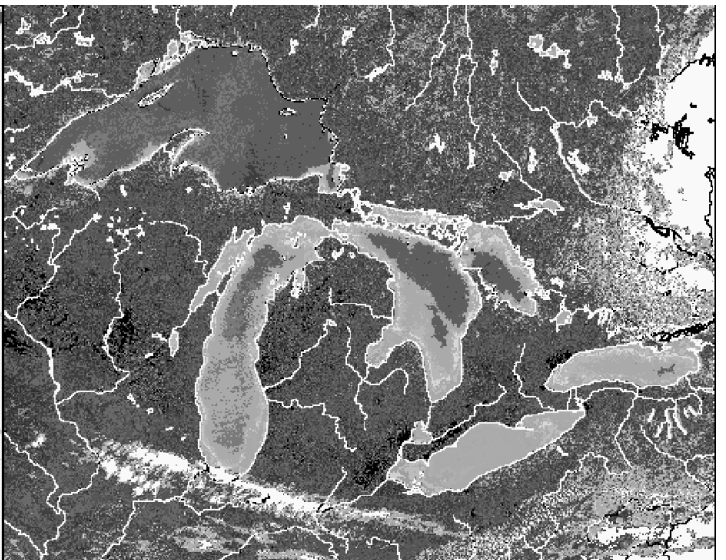
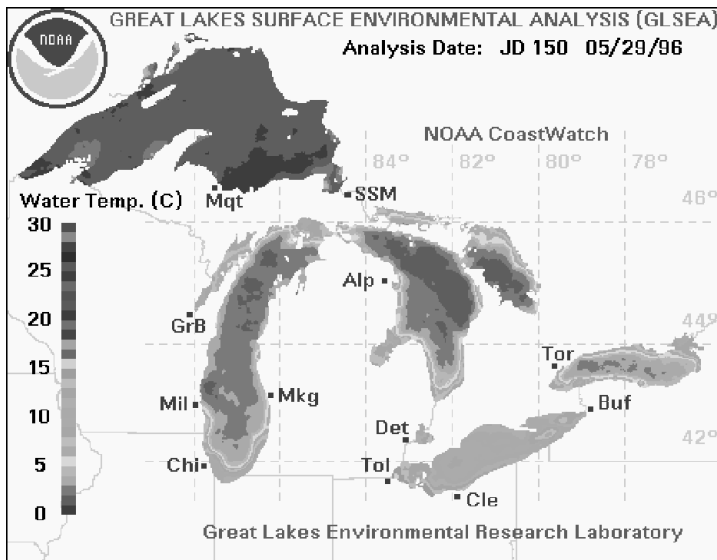


TABLE 2. Comparison of NDBC buoy daily average surface water temperatures and water temperatures derived from GLSEA for 1992–1997. *N* is the number of days for which the comparison was made. RMSD is the root mean square difference and CC is the correlation coefficient. All temperatures are °C.

Buoy Number	N	Average Buoy Temperature	Average GLSEA Temperature	Mean Difference	RMSD	CC
45001	1132	5.67	5.32	0.35	1.10	0.97
45002	1280	10.32	9.93	0.39	1.33	0.98
45003	1201	9.01	8.69	0.32	1.50	0.97
45004	1120	5.51	5.22	0.28	1.10	0.96
45005	1155	17.56	18.06	-0.50	1.76	0.96
45006	1132	7.09	7.12	-0.04	1.31	0.97
45007	1348	11.93	12.27	-0.34	1.50	0.98
45008	1072	11.95	11.79	0.17	1.35	0.98

TABLE 3. Cloud masking techniques and satellite imagery used in Great Lakes Surface Environmental Analysis automated production from 1994–97. C1/C2 indicates the cloud masking technique based on AVHRR channel 1 and 2 only was used. CW indicates the CoastWatch cloud mask product was used.

Dates	Cloud Mask		NOAA Satellite			Pass(es)	
	C1/C2	CW	11	12	14	Day	Night
1/5/94–9/13/94	X		X			X	
9/14/94–10/24/94	X			X		X	
10/25/94–3/29/95		X		X		X	X
3/30/95–4/23/95		X		X	X	X	X
4/24/95–present		X			X	X	X

cal mean for each lake and the average departure for all five lakes.

DISCUSSION AND CONCLUSIONS

The RMS deviations of 1.1 to 1.8°C between GLSEA derived surface water temperature and daily averaged NDBC buoy temperature shown in Figure 3 and Table 2 are comparable to or slightly greater than differences of 0.79 to 1.56°C reported between instantaneous (hourly) buoy measurements and temperatures derived from individual satellite images (Schwab *et al.* 1992, Strong 1974). The RMS deviations of 1.1 to 1.8°C provide an indication of the added uncertainty introduced by the compositing process. This should still be considered very good agreement, given that a large number of the GLSEA maps correspond to days when the individual satellite images were cloud covered at the buoy location. Nevertheless, there are proba-

bly several improvements which could be incorporated into the GLSEA processing to improve the agreement, including more sophisticated cloud masking and better screening for anomalous temperature values.

Figures 6 and 7 demonstrate the usefulness of the GLSEA compositing procedure on partly cloudy days, which are the norm for the Great Lakes region during most of the year. In cloud-free areas, the latest water temperature information from the AVHRR satellite imagery is incorporated into the composite, while in cloud covered areas, water temperatures from the previous composite are used. In this way, a full map of the spatial distribution of surface water temperature is obtained in near real-time. It should be noted that because of the high occurrence of cloud cover in the Great Lakes most maps contain a mixture of current and previous data.

One application of the GLSEA product is the es-

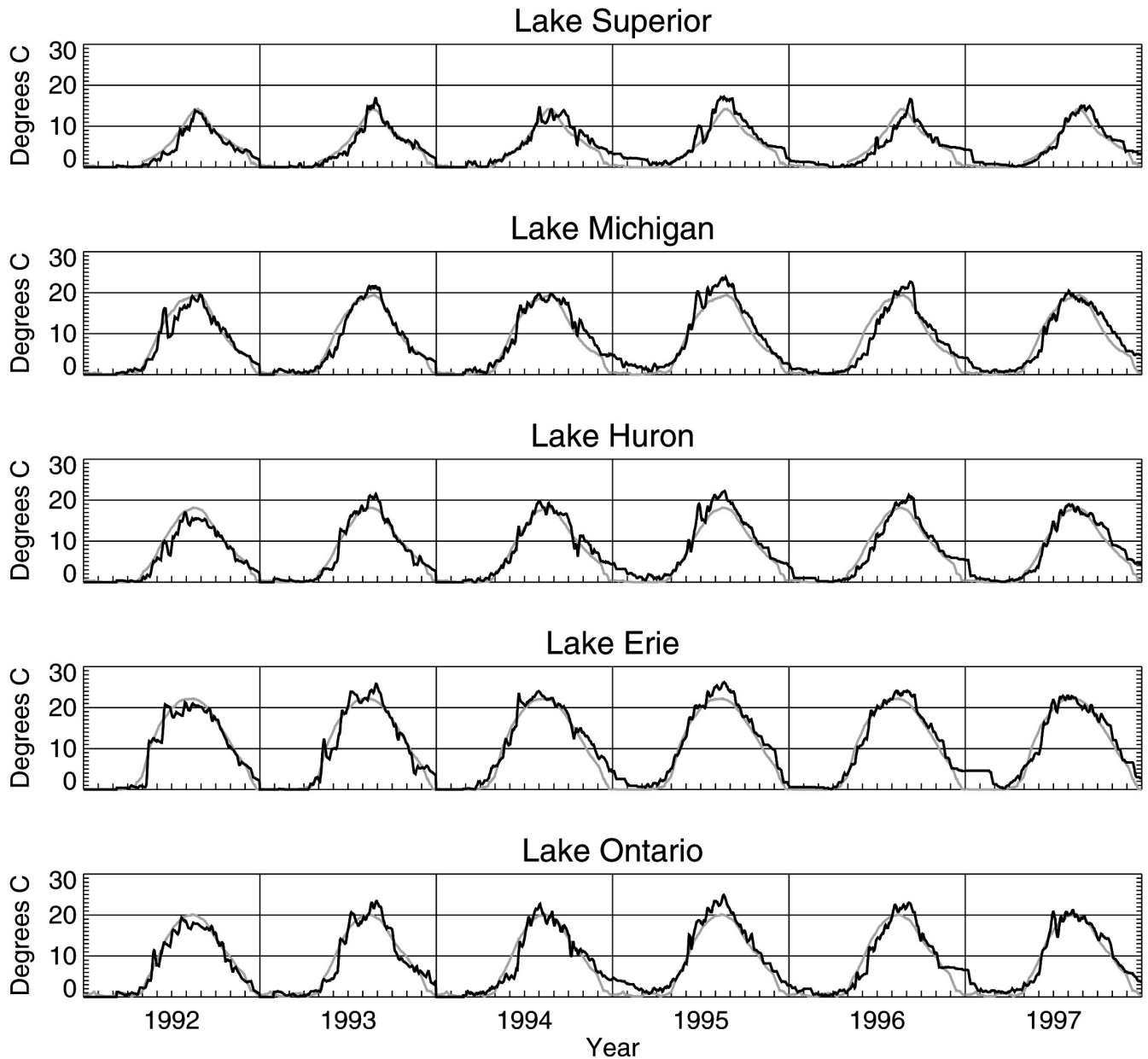


FIG. 9. Daily mean surface water temperature for 1992–1997 from GLSEA (black line) and climatological annual mean surface water temperature cycle from Schneider et al. (1993) (gray line).

timation of lake average surface water temperatures for each lake on a daily basis, as shown in Figure 9. This figure also illustrates one of the limitations of the GLSEA product in that even the compositing technique cannot continue to provide realistic estimates of lake surface temperature during extended periods of cloud cover. During an extended period of cloud cover, the GLSEA temperature for a par-

ticular lake does not change very much, until new thermal imagery becomes available, when the average lake temperature can change abruptly. This is particularly evident in the spring and fall periods when lake temperatures are changing most rapidly, for instance in the spring of 1992 in Lake Erie and the fall of 1996 for all lakes. The addition of a post-processing feature to the GLSEA procedure is

TABLE 4. Departure of GLSEA-derived water surface temperature (%C) from climatological values of Schneider et al. (1993)

Lake	1992	1993	1994	1995	1996	1997	All years
Superior	-0.69	-0.04	0.74	1.65	0.11	0.75	0.42
Michigan	-0.53	0.06	0.97	1.86	0.13	0.75	0.54
Huron	-1.08	0.26	0.70	1.72	0.36	0.73	0.45
Erie	-0.75	0.04	1.19	1.55	0.67	1.09	0.63
Ontario	-0.63	0.11	0.08	1.80	0.55	0.94	0.48
All lakes	-0.74	0.09	0.74	1.72	0.36	0.85	0.50

under consideration that would produce improved water temperature maps for the previous week or month by interpolating temperatures in time during extended periods of cloud cover. This procedure has not yet been implemented.

The temperature anomaly graph in Figure 10 illustrates the potential usefulness of the GLSEA lake average surface water temperature as an indicator of climatological conditions. In Figure 10, lake temperatures in 1992 are seen to be up to 4°C below the Schneider *et al.* (1993) climatological values in all lakes. In 1995, water temperatures were 2 to 3°C above climatological values during most of the year. GLSEA temperatures appear to be above the climatological values every winter, but this is an artifact caused by inadequate handling of ice cover in the GLSEA procedure. This deficiency will be rectified when digital ice maps are incorporated from the National Ice Center into the GLSEA product.

There is also a persistent tendency for the GLSEA temperature to be lower than the Schneider *et al.* (1993) climatology during the springtime warming period in almost all years in all lakes. This difference may be because of the procedures Schneider *et al.* (1993) used to develop the climatological water temperature maps. By averaging water temperature data from several years, the rapid warming that occurs in the springtime is smoothed out over a longer period such that in years when the warming occurs later than normal, the climatological temperature for a particular day is usually higher than the actual lake temperature. In years when the spring warming occurs earlier than normal, the climatological temperature can be lower than the actual temperature, but the difference is usually less than in the case of late warming. This effect can be seen graphically by comparing the JD

150 climatological surface water temperature map from Schneider *et al.* (1993) (Fig. 11) to the GLSEA product for that day in 1996 (Fig. 4). There is a much more continuous temperature gradient from nearshore to offshore regions in the climatological map (Fig. 11) than in the GLSEA map (Fig. 4). In the GLSEA map (Fig. 4), temperatures are more uniform in the deeper regions of each lake than in the climatological map (Fig. 11). The climatological averaging process tends to eliminate the sharp thermal transition that occurs across the "thermal bar" region during this time of year, mainly because warming occurs earlier in some years and later in others, and the temporal averaging tends to smooth out the spatial gradients. The GLSEA procedure provides a more realistic depiction of the temperature distribution during this period.

As mentioned above, information about ice cover will be added to the GLSEA product beginning in the 1998 to 99 ice season. Digital ice cover maps from the National Ice Center will be incorporated by indicating which GLSEA pixels contain ice cover in five ranges: < 11%, 11–39%, 40–70%, 71–99%, and 100%. The ice maps are based on satellite imagery, aircraft reconnaissance, and surface observations which are compiled by the National Ice Center and used to produce a new map for the Great Lakes two to three times a week during the ice season (Bertoia *et al.* 1998). A digital version of the latest ice analysis chart will be downloaded and incorporated into the daily GLSEA during the ice season. Besides providing a combined digital map of water temperature and ice cover, it is believed that this procedure will also considerably improve estimates of mean lake surface temperature during the winter months.

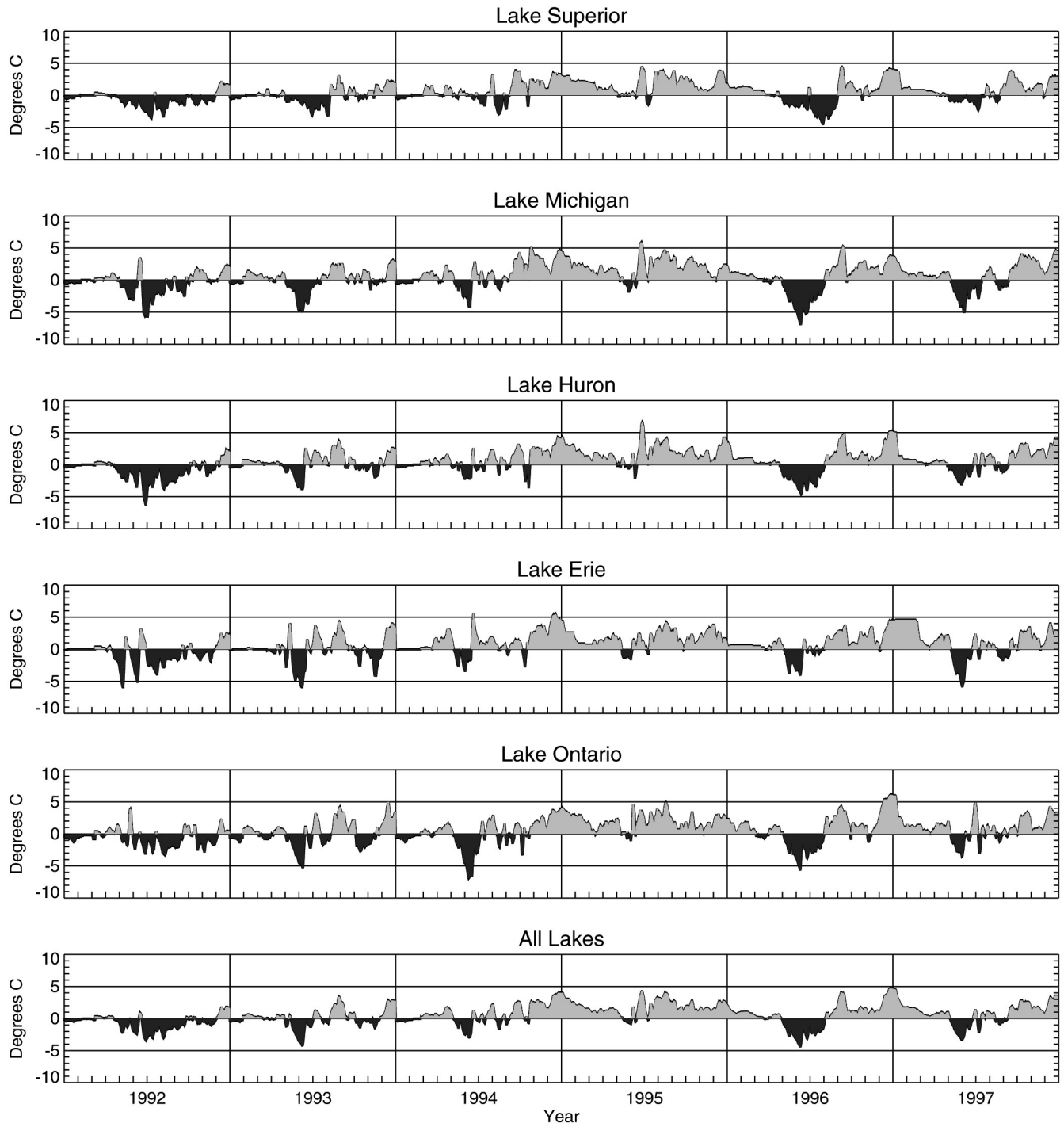


FIG. 10. Departure of GLSEA daily mean surface water temperature from climatological mean surface water temperature of Schneider et al. (1993). Gray shading indicates lake temperatures greater than climatology, black shading values less than climatology.

REFERENCES

- Anderson, D.V., and Rodgers, G.K. 1963. A synoptic survey of Lake Superior. In *Proc. 6th Conf. Great Lakes Res.*, pp. 79–111, Internat. Assoc. Great Lakes Res.
- Assel, R.A., Quinn, F.H., Leshkevich, G.A., and Bolsenga, S.J. 1983. *NOAA Great Lakes Ice Atlas*. Great Lakes Env. Res. Lab., Ann Arbor, MI.
- Ayers, J.C. 1965. *The Climatology of Lake Michigan*. University of Michigan, Great Lakes Res. Div. Publication 12.
- Bertoia, C., Falkingham, J., and Fetterer, F. 1998. Polar SAR data for operational sea ice mapping. In *Recent Advances in the Analysis of SAR Data of the Polar Oceans*, ed. R. Kwok and C. Tsatsoulis, pp. 201–234. Berlin, Springer Verlag.
- Bolgrien, D.W., and Brooks, A.S. 1992. Analysis of thermal features of Lake Michigan from AVHRR satellite images. *J. Great Lakes Res.* 18(2):259–266.
- Bordes, P., Brunel, P., and Marsouin, A. 1992. Automatic adjustment of AVHRR navigation. *J. Atmos. and Oceanic Technology* 9:15–27.
- Church, P.E. 1945. *The annual temperature cycle of Lake Michigan, II. (Spring warming and summer stratification period 1942)*. Dept. of Meteor. Univ. of Chicago MR 18.
- Grumblatt, J.L. 1976. *Great Lakes water temperatures, 1966–1975*. NOAA Tech. Memo. ERL GLERL-11-1, NOAA Great Lakes Env. Res. Lab., Ann Arbor, MI.
- Hamilton, G. D. 1986. National Data Buoy Center Programs. *Bull. Amer. Meteor. Soc.* 67(4):411–415.
- Irbe, J.G. 1992. *Great Lakes surface water temperature climatology*. Atmospheric Environment Service, Canada, Climatological Studies No. 43.
- , Morcrette, J.J., and Hogg, W.D. 1979. *Surface water temperature of lakes from satellite data corrected for atmospheric attenuation*. CCC Rep. No. 79-9, Canadian Climate Center, Downsview, Ontario.
- Kidwell, K.B. 1995. *NOAA Polar Orbiter Data Users Guide*. NOAA National Environmental Satellite Data and Information Service, Washington, D.C.
- Leshkevich, G.L., Schwab, D.J., and Muhr, G.C. 1993. Satellite environmental monitoring of the Great Lakes: A review of NOAA's Great Lakes CoastWatch program. *Photogrammetric Eng. And Remote Sensing* 59(3):371–379.
- , Schwab, D.J., and Muhr, G.C. 1997. Satellite environmental monitoring of the Great Lakes: Great Lakes CoastWatch program update. *MTS J.* 30(4):28–35.
- Lesht, B.M., and Brandner, D.J. 1992. Functional representation of Great Lakes surface temperatures. *J. Great Lakes Res.* 18(1):98–107.
- Lyons, W.A. 1971. Low level divergence and subsidence over the Great Lakes in summer. In *Proc. 14th Conf. Great Lakes Res.*, pp. 467–487, Internat. Assoc. Great Lakes Res.
- Maturi, E.M., and Pichel, W.G. 1993. Cloud masking for CoastWatch satellite imagery. In *Engineering in Harmony with the Oceans, Oceans '93*, Volume II, pp.369–374.
- McCormick, M.J., and Fahnenstiel, G.L. 1998. Recent climatic trends in nearshore water temperatures in the St. Lawrence Great Lakes. *Limnology Oceanogr.* (In review)
- McFadden, J.T., and Ragotzkie, R.A. 1963. Aerial mapping of surface temperature pattern in Lake Michigan. In *Proc. 6th Conf. Great Lakes Res.*, pp. 55–58. Internat. Assoc. Great Lakes Res.
- Petterson, S., and Calabrese, P.A. 1959. On some weather influences due to warming of air by the Great Lakes in winter. *J. Meteor.* 16:646–652.
- Pyke, T.N. 1989. CoastWatch: New mission for NOAA weather satellites. *Sea Technology* 30(4):27–32.
- Schneider, K., Assel, R.A., and Croley, T.E. 1993. *Normal water temperature and ice cover of the Laurentian Great Lakes: A computer animation, data base, and analysis tool*. NOAA Tech. Memo. ERL GLERL-81, NOAA Great Lakes Env. Res. Lab., Ann Arbor, MI.
- Schwab, D.J., Leshkevich, G.A., and Muhr, G.C. 1992. Satellite measurements of surface water temperature in the Great Lakes: Great Lakes CoastWatch. *J. Great Lakes Res.* 18(2):247–258.
- Stowe, L.L., McClain, E.P., Carey, R., Pellegrino, P., Gutman, G.G., Davis, P., and Hart, S. 1991. Global distribution of cloud cover derived from NOAA/AVHRR operational satellite data. *Adv. Space Res.* 11(3):51–54.
- Strong, A.E. 1974. Great Lakes temperature maps by satellite (IFYGL). In *Proc. 17th Conf. Great Lakes Res.*, pp. 321–333. Internat. Assoc. Great Lakes Res.
- Webb, M.S. 1974. Surface temperatures of Lake Erie. *Water Resources Res.* 10:199–210.
- Weiss, M. 1970. Water surface measurement using airborne infrared techniques. In *Proc. 13th Conf. Great Lakes Res.*, pp. 978–989, Internat. Assoc. Great Lakes Res.
- Wesely, M.L. 1979. Heat transfer through the thermal skin of a cooling pond with waves. *J. Geophys. Res.* 84(C7):3696–3700.

Submitted: 23 November 1998

Accepted: 22 April 1999

Editorial handling: Paul F. Hamblin

APPENDIX A—WORLD WIDE WEB ACCESS TO COASTWATCH DATA

The compositing technique described in this paper has been applied to CoastWatch imagery since 1992 and the Great Lakes Surface Environmental Analysis (GLSEA) surface water temperature charts have been available on a daily basis on the World Wide Web since 1994. The latest GLSEA chart can be obtained from the Great Lakes CoastWatch Web site at URL <http://coastwatch.glerl.noaa.gov>. In addition, a computer animation of the previous 365 daily GLSEA charts and animations for each calendar year starting with 1992 are available in Audio Video Interleave (AVI), FLIC,

and Quicktime (QT) formats. The animations can be viewed and/or downloaded from the Great Lakes CoastWatch web site with a current web browser.

Starting in February 1999, the winter Great Lakes Ice Analysis produced and provided by the National Ice Center has been digitally overlaid on the GLSEA surface water temperature chart to show the latest ice cover concentration (%) during the winter season. In the future, the GLSEA product will include information on ice cover during the entire ice season on the Great Lakes.